

Dynamic Nonlinear Effect on Lasing in a Random Medium

B. Liu, A. Yamilov, Y. Ling, J.Y. Xu, and H. Cao*

Department of Physics and Astronomy, Northwestern University, Evanston, Illinois 60208-3112, USA
(Received 15 October 2002; published 7 August 2003)

We have studied both experimentally and numerically the dynamic effect of nonlinearity on lasing in disordered medium. The third-order nonlinearity not only changes the frequency and size of lasing modes, but also modifies the laser emission intensity and laser pulse width. When the nonlinear response time is longer than the lifetime of the lasing mode, the nonlinearity changes the laser output through modifying the size of the lasing mode. When the nonlinear response is faster than the buildup of the lasing mode, positive nonlinearity always extracts more laser emission from the random medium due to the enhancement of single particle scattering.

DOI: 10.1103/PhysRevLett.91.063903

PACS numbers: 42.25.Dd, 05.45.-a, 42.55.-f, 71.55.Jv

Over the past decade, there has been considerable interest in nonlinear optical processes in disordered media [1]. It has been shown that optical nonlinearity can modify light transport in disordered medium [2,3]. The coherent backscattering peak exhibits additional features in the presence of third-order nonlinearity [4]. Temporal fluctuation of scattered waves in nonlinear disordered medium leads to instability of the speckle pattern [5]. In those studies, to avoid absorption, the probe light frequency is far away from any resonant frequency of the nonlinear material. The nonresonant nonlinearity can be assumed to be of instantaneous response. We intend to understand the nonlinear effect in active random media. The emitted light (at the resonant frequency) experiences resonant nonlinearity, which is much stronger than nonresonant nonlinearity. Moreover, the nonlinear response time becomes finite.

Recent studies illustrate that adding gain to a disordered medium leads to lasing in the long-lived eigenmodes [6,7]. Despite the modes with long lifetime preferably being amplified, their wavefunctions are not modified by the presence of gain. However, nonlinearity can change the eigenmodes of a disordered system. In random lasers nonlinear effect is significant because spatial confinement of lasing modes results in high laser intensity.

In this Letter, we study the effect of nonlinearity on lasing in a disordered medium. The experimental evidence of the change of lasing modes is presented first. It is followed by numerical simulation of a model system with third-order nonlinearity. Our results demonstrate that nonlinearity not only modifies the frequency and size of the eigenmodes of a disordered system, but also changes laser emission intensity and laser pulse width of a random laser. The nonlinear response time plays a crucial role in the dynamic nonlinear effect on random lasing.

We used two types of random media in our experiments. One is poly(methyl methacrylate) (PMMA) sheets containing rhodamine 640 (Rh640) perchlorate dye and titanium dioxide (TiO₂) microparticles, the other is closely packed ZnO nanoparticles with average diameter

100 nm. The dye concentration in PMMA is 10 mM. The TiO₂ particles have an average diameter of 0.4 μm . The density of TiO₂ particles is $\sim 1.4 \times 10^{12} \text{ cm}^{-3}$. The PMMA sheet is optically excited by the second harmonics of a mode-locked Nd:YAG laser. The spectrum of emission from the sample is measured by a 0.5-meter spectrometer with a charge-coupled device array detector. When pump intensity exceeds the lasing threshold, discrete lasing modes emerge in the emission spectrum. As the pump intensity increases, the gain spectrum of dye molecules shifts towards longer wavelength. This redshift is caused by excited state absorption [8], and has been confirmed experimentally in neat dye solution [9]. As shown in Fig. 1, additional lasing modes appear on the long wavelength side, while some lasing modes on the short wavelength side disappear. However, individual lasing modes shift towards shorter wavelength, as marked in Fig. 1. Typically optical gain pulls the frequencies of lasing modes towards the peak of gain

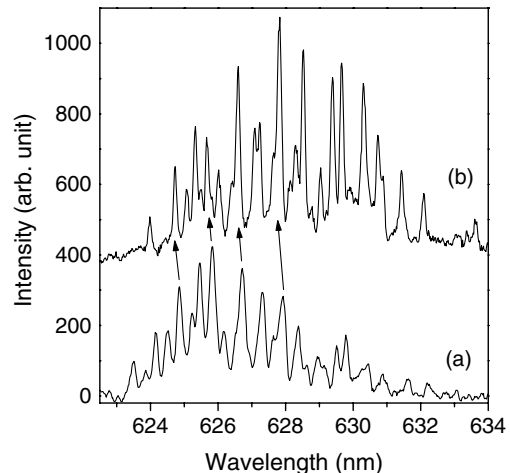


FIG. 1. Time-integrated spectra of laser emission from a PMMA sheet with dye and microparticles. The incident pump intensities are $2.0 \times 10^{12} \text{ W/m}^2$ (a), and $4.0 \times 10^{12} \text{ W/m}^2$ (b). The top spectrum is shifted vertically for clarity.

spectrum (frequency pulling effect). In our experiment, the lasing modes move in the opposite direction as the gain spectrum. This suggests the spectral shift of lasing modes is caused by nonlinearity. Nonlinear Kerr effect has been observed in a Rh640 solution containing TiO_2 particles [10]. The refractive index n changes linearly with light intensity I : $n = n_0 + n_2 I$, where n_0 is the linear refractive index, n_2 is the nonlinear Kerr coefficient. The nonlinearity is contributed mainly by dye molecules. The value of n_2 in our samples is in the range -10^{-14} to $-10^{-15} \text{ m}^2/\text{W}$. Above the lasing threshold, the excitation intensity is on the order of 10^{11} W/m^2 . Thus the change of refractive index Δn ranges from -10^{-3} to -10^{-4} . The negative sign of n_2 explains the decrease of lasing wavelengths as the pump intensity increases. The wavelength shift is in the range 0.1–1.0 nm, which is on the same order of the experimental shift.

In addition to time-integrated spectra, we measured time-resolved lasing spectra to track the spectral shift of lasing modes in time. Figure 2 shows a spectral-temporal image of laser emission from closely packed ZnO powder. The ZnO powder is optically excited by 20 ps pulses from a frequency-tripled Nd:YAG laser. Laser emission from ZnO powder is dispersed by a 0.3-meter spectrometer, then directed into a Hamamatsu streak camera. The lasing modes at a shorter wavelength are redshifted with time, while the lasing modes at a longer wavelength are blueshifted with time. The modes in the center do not shift in wavelength. For example, the mode labeled A shifts from 387.76 nm at $t = 40$ ps to 387.96 nm at $t = 130$ ps. The mode labeled B shifts from 390.69 nm at $t = 40$ ps to 390.58 nm at $t = 105$ ps. The wavelength of mode C remains nearly constant in time.

The temporal shift of lasing frequencies must result from dynamic change of the refractive index of ZnO. It is known that ZnO has a large third-order nonlinearity near its band edge [11]. The values of its third-order nonlinear

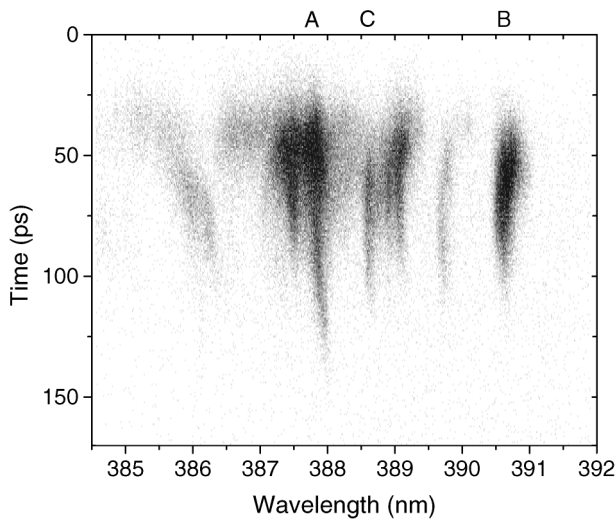


FIG. 2. A spectral-temporal image of laser emission from ZnO powder.

coefficient $\chi^{(3)}$ range from 10^{-16} to $10^{-14} \text{ m}^2/\text{V}^2$ at room temperature. The nonlinear response of ZnO is also fast: its nonlinear response time is measured to be 160 fs near band edge [12].

To understand the nonlinear effect on random lasing, we performed numerical simulation based on the finite-difference time-domain (FDTD) solution of Maxwell equations and rate equations for electronic populations [13,14]. The model system is one-dimensional simplification of the real experiment. The binary layers are made of dielectric materials with dielectric constants of $\epsilon_1 = \epsilon_0$ and $\epsilon_2 = 9\epsilon_0$, respectively. The thickness of the first layer, which simulates the gain medium, is a random variable: $a = a_0(1 + w_a \alpha)$, where $a_0 = 400$ nm, w_a describes the strength of randomness, and α is the random value in the range $[-0.5, 0.5]$. The thickness of the second layer, which simulates the nonlinear medium, is $b = b_0(1 + w_b \beta)$, where $b_0 = 100$ nm, w_b is the strength of randomness, and β is random value in the range $[-0.5, 0.5]$. For simplicity, the gain component and the nonlinear component are separated in our model. The dynamics of electronic populations in the gain layers is described by four-level rate equations, with parameters similar to those in Ref. [14]. In the nonlinear layers, the third-order nonlinearity is described by the nonlinear polarization [15] $P_{NL}(x, t) = \epsilon_0 \chi^{(3)} E(x, t) \int_{-\infty}^{\infty} g(t - \tau) |E(x, \tau)|^2 d\tau$, where $\chi^{(3)}$ is the third-order susceptibility and E is the electric field. The casual response function $g(t - \tau) = (1/\tau_0) \exp[-(t - \tau)/\tau_0]$ for $t \geq \tau$, and $g(t - \tau) = 0$ for $t < \tau$, where τ_0 is the nonlinear response time. To incorporate the nonlinearity with finite response time into the FDTD algorithm, we introduce a new function $G(x, t) \equiv \int_{-\infty}^{\infty} g(t - \tau) |E(x, \tau)|^2 d\tau = (1/\tau_0) \int_0^t e^{-(t-\tau)/\tau_0} |E(x, \tau)|^2 d\tau$. The differential equation for $G(x, t)$ can be derived as

$$\frac{dG(x, t)}{dt} = -\frac{G(x, t)}{\tau_0} + \frac{|E(x, t)|^2}{\tau_0}. \quad (1)$$

The electric field E is related to the electric displacement D by accounting for the linear polarization P_L and the nonlinear polarization P_{NL} : $E(x, t) = [D(x, t) - P_L(x, t) - P_{NL}(x, t)]/\epsilon_0 \epsilon_\infty$. Since $P_L = \epsilon_0 \chi^{(1)} E$ and $P_{NL} = \epsilon_0 \chi^{(3)} E G$, the effective dielectric constant $\epsilon(x, t) = \epsilon_\infty + \chi^{(1)} + \chi^{(3)} G(x, t)$, where $\chi^{(1)}$ is the linear susceptibility. When light frequency is far from any resonant frequency, $\tau_0 \rightarrow 0$, the nonlinearity becomes instantaneous. $g(t - \tau) = \delta(t - \tau)$, and $G(x, t) = |E(x, t)|^2$. The nonlinear dielectric constant $\epsilon = \epsilon_L + \chi^{(3)} |E|^2$, where $\epsilon_L = \epsilon_\infty + \chi^{(1)}$ is the linear dielectric constant.

To simulate pulsed pumping, the external pumping term in the rate equations represents a Gaussian pulse of width 20 ps: $P_r(t) = 2 \times 10^8 e^{-\ln 2 (t-t_0)^2/t_0^2} / \text{s}$, where $t_0 = 10$ ps. We first turn off the nonlinearity by setting $\chi^{(3)} = 0$ to simulate lasing in linear random medium. The random structure consists of 50 layers with $w_a = w_b = 0.9$. The radiative transition of the four-level system is

centered at $\lambda_a = 389$ nm with 7 nm spectral width. We choose the pumping rate so that only one mode lases. The frequency of the lasing mode does not exhibit any noticeable change during the lasing process. Next we include the nonlinearity. We choose the value of $\chi^{(3)}$ to be $1.2 \times 10^{-16} \text{ m}^2/\text{V}^2$, close to the measured value for ZnO at room temperature [12]. Figure 3 plots temporal evolution of lasing spectra obtained by Fourier transform of the electric field in 2.6 ps intervals. For negative (positive) nonlinearity $\chi^{(3)} < 0$ ($\chi^{(3)} > 0$), the lasing mode first shifts towards shorter (longer) wavelength as the laser intensity increases, then shifts to longer (shorter) wavelength as the laser intensity decreases. These results can explain qualitatively the experimental observation of lasing frequency shift with time. As shown in Fig. 2, the laser pulses in ZnO powder rise quickly then decay slowly. The rising edge of the laser pulses is too short to detect a temporal shift of the lasing frequency. However, the falling edge of the laser pulses is long enough to observe noticeable shift of lasing frequency with time. In the presence of population inversion, $\chi^{(3)}$ is positive (negative) for photon frequency below (above) the band gap. For the lasing modes whose frequencies are below (above) the ZnO band edge, since $\chi^{(3)} > 0$ ($\chi^{(3)} < 0$), they shift towards shorter (longer) wavelength in the falling edge as in Fig. 3(b) (Fig. 3(a)). For the lasing modes at the band edge, $\chi^{(3)} \approx 0$; thus their frequencies remain nearly constant with time. The wavelength shift in our calculation is $\sim 1\text{--}2 \text{ \AA}$, close to the experimental value.

The spatial size of lasing modes also changes in the presence of third-order nonlinearity. When only one mode lases, the size of the lasing mode can be characterized by the inverse partition ratio $r(t) = (\int |E(x, t)|^2 dx)^2 / \int |E(x, t)|^4 dx$. Figure 4 plots $r(t)$ of one lasing mode (the same one as in Fig. 3) in both linear and nonlinear cases. For this mode, when $\chi^{(3)} > 0$ ($\chi^{(3)} < 0$), $r(t)$ increases (decreases) during the lasing period. We repeat the calculation for lasing modes in many random

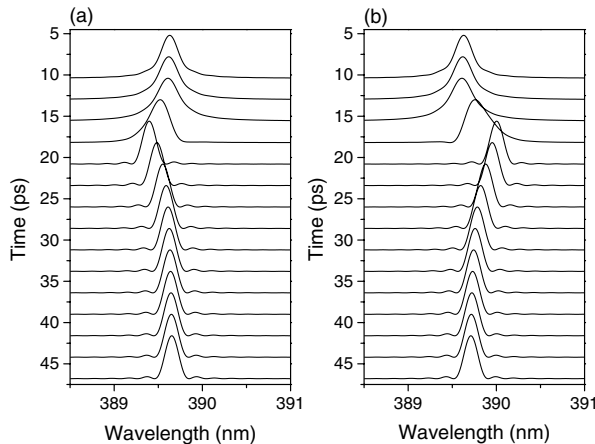


FIG. 3. Temporal evolution of lasing spectra calculated for (a) $\chi^{(3)} = -1.2 \times 10^{-16} \text{ m}^2/\text{V}^2$, (b) $\chi^{(3)} = 1.2 \times 10^{-16} \text{ m}^2/\text{V}^2$.

configurations. However, we do not find any definite relation between the sign of the nonlinearity and the size change of the lasing modes. This is understandable because the eigenmodes of a disordered medium are chaotic; i.e., a small change of the medium at one point in space already leads to a large unpredictable change of the eigenmode structure [16].

Optical nonlinearity not only changes the frequency and size of lasing modes, but also modifies the intensity and duration of laser pulses. The change of laser output is sensitive to the nonlinear response time τ_0 . We calculate the laser pulses by fixing the value of $\chi^{(3)}$ and varying τ_0 . Figure 5 plots the total laser emission energy $U(t) = (1/2) \int \epsilon_0 \epsilon |E(x, t)|^2 dx$ for $\chi^{(3)} = \pm 1.2 \times 10^{-16} \text{ m}^2/\text{V}^2$. We first set τ_0 equal to the experimentally measured value (160 fs) of passive ZnO near its band edge [12]. For positive (negative) $\chi^{(3)}$, the laser pulse becomes weaker (stronger) than that in the linear case. Next we repeat the calculation with smaller τ_0 since the nonlinear response time is shortened in the presence of stimulated emission. As shown in Fig. 5, when $\tau_0 = 6.5$ fs, the behavior of the laser pulse becomes totally different. For positive (negative) $\chi^{(3)}$, the laser pulse becomes stronger (weaker) and longer (shorter) than that in the linear case.

From the calculation of many random lasing modes, we conclude that the effect of nonlinearity on laser pulse intensity and width depends on the relative magnitude of two time scales. One is the nonlinear response time τ_0 , and the other is the lifetime τ_c of the lasing mode in the passive medium. τ_c can be obtained by launching a pulse at the frequency of the lasing mode in the passive medium and observing the temporal decay of the electric field [6]. When τ_0 is longer than τ_c , the change of laser pulse intensity and width is related to the size change of the lasing mode. If the size of the lasing mode decreases (increases) in the presence of nonlinearity, light confinement gets better (worse). The decrease (increase) of light leakage is equivalent to an increase (decrease) of

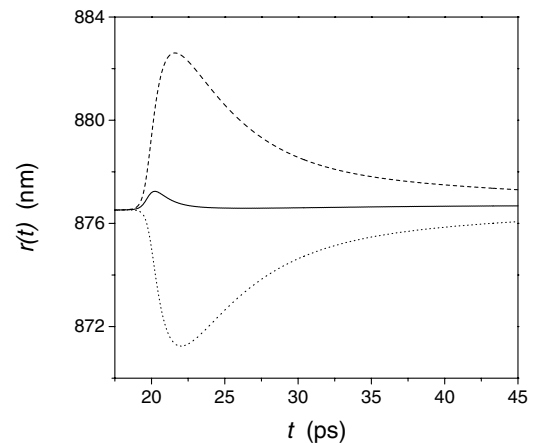


FIG. 4. Spatial size of the lasing mode $r(t)$ calculated for $\chi^{(3)} = 0$ (solid line), $\chi^{(3)} = -1.2 \times 10^{-16} \text{ m}^2/\text{V}^2$ (dotted line), and $\chi^{(3)} = 1.2 \times 10^{-16} \text{ m}^2/\text{V}^2$ (dashed line).

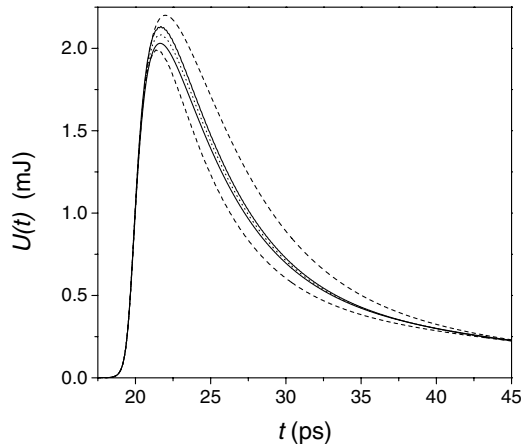


FIG. 5. Laser emission energy $U(t)$ calculated for (from top to bottom) $\chi^{(3)} = 1.2 \times 10^{-16} \text{ m}^2/\text{V}^2$ and $\tau_0 = 6.5 \text{ fs}$; $\chi^{(3)} = -1.2 \times 10^{-16} \text{ m}^2/\text{V}^2$ and $\tau_0 = 160 \text{ fs}$; $\chi^{(3)} = 0$; $\chi^{(3)} = 1.2 \times 10^{-16} \text{ m}^2/\text{V}^2$ and $\tau_0 = 160 \text{ fs}$; $\chi^{(3)} = -1.2 \times 10^{-16} \text{ m}^2/\text{V}^2$ and $\tau_0 = 6.5 \text{ fs}$.

the quality factor of the random cavity. Hence, lasing lasts longer (shorter), and laser emission is stronger (weaker). When τ_0 is shorter than τ_c , the change of laser output depends only on the sign of $\chi^{(3)}$; i.e., positive (negative) nonlinearity always extracts more (less) laser emission from the random medium at the same pumping rate. This is because when the nonlinear response is faster than the buildup of the lasing mode, the lasing mode cannot respond fast enough to the nonlinear refractive index change. The phase of scattered light changes quickly due to rapid change of refractive index with intensity. The absence of constant phase relations among light waves scattered by different particles undermines the interference effect. Hence, the effect of single particle scattering becomes dominant over the collective effect of many particle scattering. For $\chi^{(3)} > 0$ ($\chi^{(3)} < 0$), the refractive index contrast of the binary layers increases (decreases) as the laser intensity increases. Light scattering of a single particle becomes stronger (weaker). The increase (decrease) of scattering strength results in more (less) efficient lasing, i.e., higher (lower) laser intensity and longer (shorter) lasing period.

In conclusion, we demonstrate that nonlinear refraction not only changes the frequency and size of random lasing modes, but also modifies the laser emission intensity and laser pulse duration. The nonlinear effects in random lasers are quite similar to those in conventional lasers and amplifiers [17,18]. However, the nonlinear response time plays a crucial role in random lasers: it determines how nonlinearity affects the lasing process, either through single particle scattering or collective scattering of many particles.

We acknowledge Dr. A. L. Burin and S.-H. Chang for stimulating discussions. This work is supported partially by the National Science Foundation under Grant No. DMR-0093949 and the David and Lucille Packard Foundation.

*Email address: h-cao@northwestern.edu

- [1] V.M. Shalaev, *Nonlinear Optics of Random Media* (Springer-Verlag, Berlin, 1999).
- [2] G.B. Al'tshuler, V.S. Ermolaev, K.I. Krylov, A.A. Manenkov, and A.M. Prokhorov, *J. Opt. Soc. Am. B* **3**, 660 (1986).
- [3] R. Bressoux and R. Maynard, *Europhys. Lett.* **50**, 460 (2000).
- [4] V.M. Agranovich and V.E. Kravtsov, *Phys. Rev. B* **43**, 13 691 (1991); A. Heiderich, R. Maynard, and B. A. van Tiggelen, *Opt. Commun.* **115**, 392 (1995).
- [5] S. E. Skipetrov and R. Maynard, *Phys. Rev. Lett.* **85**, 736 (2000).
- [6] C. Vanneste and P. Sebbah, *Phys. Rev. Lett.* **87**, 183903 (2001); X. Jiang and C.M. Soukoulis, *Phys. Rev. E* **65**, R25 601 (2002).
- [7] H. Cao, Y. Ling, J.Y. Xu, and A.L. Burin, *Phys. Rev. E* **66**, R25 601 (2002).
- [8] E. Sahar and D. Treves, *IEEE J. Quantum Electron.* **13**, 962 (1977); P. Venkateswarlu, M.C. George, Y.V. Rao, H. Jagannath, G. Chakrapani, and A. Miahnahri, *Pramana* **28**, 59 (1987).
- [9] W.L. Sha, C.-H. Liu, and R.R. Alfano, *Opt. Lett.* **19**, 1922 (1994).
- [10] R. E. de Araujo and A. S. L. Gomes, *Phys. Rev. A* **57**, 2037 (1998).
- [11] H. Kalt, V.G. Lyssenko, R. Renner, and C. Klingshirn, *J. Opt. Soc. Am. B* **2**, 1188 (1985); J.N. Ravn, *IEEE J. Quantum Electron.* **28**, 315 (1992).
- [12] W. Zhang, H. Wang, K. S. Wong, Z. K. Tang, and G. K. L. Wong, *Appl. Phys. Lett.* **75**, 3321 (1999).
- [13] A. Taflove and S.C. Hagness, *Computational Electrodynamics: the Finite-Difference Time-Domain Method* (Artech House, Boston, 2000).
- [14] C. M. Soukoulis, X. Jiang, J.Y. Xu, and H. Cao, *Phys. Rev. B* **65**, R41 103 (2002).
- [15] R.W. Ziolkowski and J. B. Judkins, *J. Opt. Soc. Am. B* **10**, 186 (1993); R. M. Joseph and A. Taflove, *IEEE Trans. Antennas Propagat.* **45**, 364 (1997).
- [16] P. A. Mello and S. Tomsovic, *Phys. Rev. B* **46**, 15 963 (1992); C.W.J. Beenakker, *Rev. Mod. Phys.* **69**, 731 (1997); H.-J. Stockmann, *J. Mod. Opt.* **49**, 2045 (2002).
- [17] N. A. Olsson and G. P. Agrawal, *Appl. Phys. Lett.* **55**, 13 (1989); G. P. Agrawal and N. A. Olsson, *Opt. Lett.* **14**, 500 (1989).
- [18] P.J. Delfyett, Y. Silberberg, and G. A. Alphonse, *Appl. Phys. Lett.* **59**, 10 (1991); A. Dienes, J.P. Heritage, M.Y. Hong, and Y.H. Chang, *Opt. Lett.* **17**, 1602 (1992); Y.-H. Liao and H.G. Winful, *Opt. Lett.* **21**, 471 (1996).